A Coherent OFDM Switching System for Flexible Optical Network Configuration

Alfred Ebberg, Reinhold Noé, Lothar Stoll, and Robert Schimpe, *Member, IEEE*

Abstract— A coherent optical switching node based on the combination of a frequency conversion stage with a space switching matrix is proposed for flexible interconnection of future integrated broad-band communication networks. The basic system concept is presented together with the architecture of a demonstrator, which allows to study the functionality available in future networks. The major subsystems and components of the demonstrator are described, and experimental results concerning frequency stabilization, frequency switching, and space switching are presented.

I. INTRODUCTION

THE interconnection of future optical networks will require a degree of capacity and rearrangement capability that may be considerably higher than expected hitherto. The (time-dependent) allocation of transmission capacity on demand between two locations may serve as one example for the raised requirements network operators will be confronted with in the future. Since the total capacity of a network or a link will always be limited by the amount of hardware available for switching and transmission purposes a better utilization of the available resources by a flexible and traffic-dependent allocation of the hardware is highly desirable.

Coherent optical multicarrier techniques favorably combine the flexibility and upgradability necessary to meet the above mentioned requirements. The capacity of an optical link using coherent optical multicarrier techniques can easily be increased by orders of magnitude, if required. This is achieved in an evolutionary manner by increasing the number of optical carriers, without having to raise the bitrate per carrier to a value that would be difficult to handle electronically. Optical carriers can easily be regrouped and rerouted which leads to a flexible capacity of the optical link according to traffic demands. In this way the available hardware in the switching node can be allocated most economically.

Compared with direct detection, coherent systems offer a superior frequency selectivity; being able to operate with channel spacings of just a few gigahertz they use the available bandwidth very efficiently. This feature becomes especially important if the system contains cascaded optical amplifiers which tend to significantly reduce the available bandwidth.
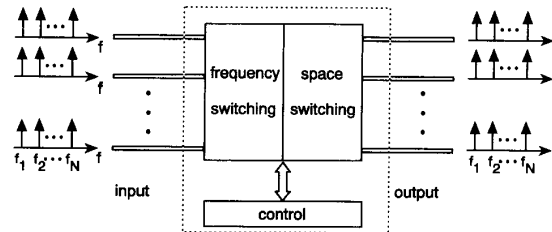
Fig. 1. Principle of an OFDM switching node comprising a frequency conversion and a space switching stage.

In order to fulfill future network requirements, coherent OFDM switching nodes consisting of a combination of frequency conversion stages and space switching stages have been proposed [1]. Within such a switching node each input signal can be switched to each output fiber and to a desired unoccupied output carrier frequency. In principle the space switching function can also be performed by stages consisting of frequency converters only [2]. An alternative architecture for a combined space and wavelength optical switching fabric is based on the MONET concept [3]. Recently a multi-stage frequency division switching node with very efficient use of the available hardware has been proposed [4].

In this paper we present a concept for a coherent OFDM switching node consisting of tunable transmitters and coherent receivers in combination with advanced integrated-optic space switching matrices. The various subsystems of the planned demonstrator are described and a number of experimental results obtained with fully engineered coherent transmission equipment [5] is presented.

II. SYSTEM ARCHITECTURE

A. Principle

The principle of the proposed coherent OFDM switching node is shown in Fig. 1. It comprises N input and N output fibers connected by a frequency- and a space switching stage. Each of the input and output fibers carries a frequency comb of M optical carriers. The possible capacity of such a node can be calculated to 1 Tb/s, assuming $M = 50$ optical carriers, each modulated at 2.5 Gb/s, and $N = 8$ fibers at the input and output. It is interesting to note that these figures could be achieved using components which are available already today (tunable lasers [6], [7], switching matrices [8], etc.).

The schematic of the planned demonstrator is shown in Fig. 2. Three tunable optical FSK transmitters TX1 $\cdots$ TX3

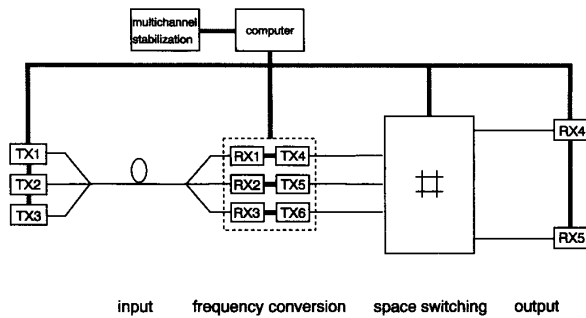input   frequency conversion   space switching   output

Fig. 2. Principle of the planned OFDM switching demonstrator.

serve as data sources at 155 Mb/s. We use Manchester coding [9] to overcome the nonuniform frequency response of the transmitter lasers. The frequency conversion stage consists of three FSK heterodyne receivers, each of which is tuned to one of the incoming carriers, and three tunable optical transmitters. Clock and data signals are regenerated in the receivers and directly fed to the transmitters. The optical outputs of the transmitters are connected to the space switching stage where the desired output fiber is selected. Each output fiber is terminated by a coherent receiver in order to allow bit error rate measurements. The frequencies of the various transmitters are stabilized by a multichannel stabilization unit. Overall control of the demonstrator is performed by a personal computer.

In the following sections the individual subsystems of the demonstrator are described and first experimental results are presented.

B. Frequency Switching Stage

The frequency switching stage converts the optical carrier frequency of one among possibly many input channels to a desired output frequency. As already mentioned it will finally consist of three tunable optical heterodyne receivers and three tunable FSK transmitters. This is presently the method of choice because coherent equipment has reached a high degree of engineering level worldwide. No tunable optical filters are required. The inherent signal regeneration is also highly welcome.

In contrast, the all-optical frequency conversion is still in a laboratory state. Its conversion efficiency is still relatively low, at least when compared to about 50 dB (and more) of signal gain achieved in coherent repeaters. In particular, all-optical frequency converters need a very individual device characterization and their performance varies widely as a function of polarization and of frequency separation between input and output signals [10]-[13]. In many cases the use of frequency-stabilized narrow-band optical filters after the frequency conversion stage is imperative in order to suppress unwanted mixing products. If conversion of one among many input channels is desired, optical filters are required at the converter input, too. Possible linewidth increase of the optical carriers caused by all-optical frequency conversion can be a problem for modulation formats such as FSK and DPSK.

Furthermore the inversion of the data in the case of frequency downconversion may cause additional problems. A promising technique for all optical frequency conversion is based on the gain saturation effect in semiconductor optical amplifiers. Broadband frequency shifting of ASK signals at datarates up to 2.5 Gb/s has been demonstrated using single [14], [15] or multisection [16] devices. Optical filters at the output of the frequency conversion stage, however, are indispensible. Very recently frequency conversion of CPFSK signals at 4.8 Gb/s using a DBR laser wavelength converter has been reported [17]. The principle has potential for high datarates, however a certain frequency offset between the input and output signal is necessary in order to avoid injection locking or detrimental effects due to the presence of the bragg grating. As a compensation for the above mentioned drawbacks all-optical frequency conversion offers the advantage of being fully transparent to the incoming signals.

In our demonstrator tuning of the receivers is performed electronically by tunable twin-guide local oscillator lasers [6], whereas the transmitters are essentially tuned thermally. Polarization handling in the receivers is performed using either polarization diversity or data-induced polarization switching (DIPS). In our case DIPS is implemented at the receiver side to allow coexistence of both schemes. Details of the receiver architecture and more information on polarization handling schemes are found in [18] and references contained therein. It should be noted, that DIPS, whether implemented in the transmitter or in the receiver, is a self-consistent system alternative to the 'traditional' polarization handling methods, i.e., endless control and diversity. A potential difficulty of DIPS is the automatic channel acquisition. Since mark and space frequencies of the optical FSK signal are received with orthogonal polarizations, the two FSK spectral lobes may fade in antiphase. If one lobe disappears, the spectrum is still held in place in the receiver by an automatic frequency control (AFC) that uses a frequency discriminator with two zero crossings of equal slope polarities at the desired mark and space intermediate frequencies [19].

For channel locking, we have developed an automatic channel acquisition routine, that takes advantage of the spectral asymmetry of the remaining lobe, caused by the finite transition time between mark and space frequencies, and by the polarization dispersion of the birefringent fiber that generates DIPS. By recording up to 15 up and down sweeps of the LO frequency in the vicinity of the signal frequency correct channel locking under all circumstances was achieved. Other than in DIPS receivers, the IF spectrum of a received channel is always symmetric in polarization diversity receivers. One LO sweep is sufficient to identify the spectral position of a channel accurately, and channel acquisition is therefore completed in a shorter time than in DIPS receivers.

So far we have completed several fully engineered coherent 140 Mb/s FSK transmitters and receivers, based on both DIPS [5] and polarization diversity. The power budget is 51.9 dB worst case, while the best transmitter with a power of +5.2 dBm and the best receiver with a sensitivity of < −56 dBm would allow for a 61.2 dB power budget. The common tuning range of the receivers is 148 GHz which allows 25 channels to
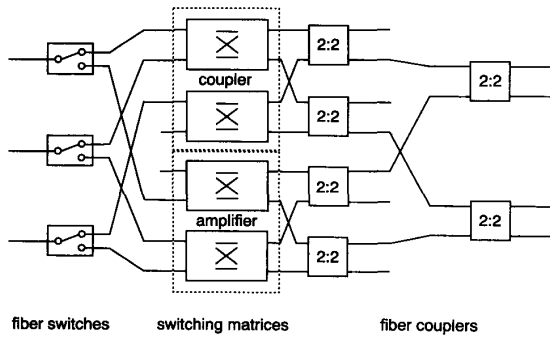
Fig. 3. Principal layout of space switching stage.

Fig. 4. Optical switching matrix based on directional couplers. (a) principle layout, (b) realized chip, (c) infrared image of matrix output.

be transmitted while staying above the minimum permissible channel spacing of 5 GHz. This number can be explained to be the applied FSK deviation (1.2 GHz) plus twice the mean IF (2 × 1.2 GHz), in order to avoid image band interference, plus a margin (1.4 GHz) that is necessary to separate adjacent channels. For the final demonstrator very similar equipment, upgraded to 155 Mb/s, will be employed.

C. Space Switching Stage

For the construction of the space switching stage a variety of options exists. Optical fiber switches are commercially available today. The switching speed of these devices is limited to a few ms which is not regarded as a serious drawback for the above mentioned application of network reconfiguration. However, the reliability of moving parts remains questionable. Switching matrices in LiNbO$_3$ have been a research topic for a long time. Meanwhile a polarization independent 8 × 8 LiNbO$_3$ switching matrix has been reported [8]. An attractive alternative are three-dimensional space switches with free-space propagation. A switching matrix as large as 128 × 128 has recently been realized using liquid crystal spatial light modulators [20].

In the demonstrator setup advanced integrated-optical switching matrices in InP will be used.

The principal layout of the space switching stage is shown in Fig. 3. It comprises four 2 × 2 integrated optical switching matrices of two different types. Either directional coupler switches, or optical amplifiers in a gate switching matrix perform the desired function. We use two different types of matrices in order to study their potential impact on system performance. The outputs of the 2 × 2 matrices are combined by 2 × 2 fiber directional couplers. The fiber switches at the inputs are used to select the desired type of switching matrix.

1) Directional Coupler Matrix: The principle of the matrix based on directional coupler switches is shown in Fig. 4. It contains two crossbar switches, two combiners, interconnecting and crossing waveguides. Each of the two input ports can be switched independently from the other to one of the two output ports resulting in four possible switching states.

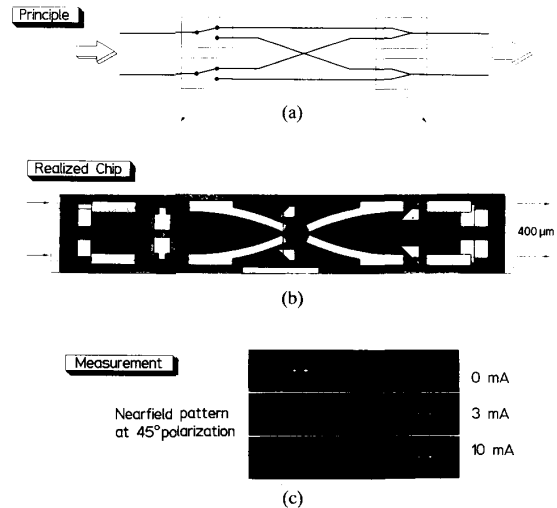The switching matrix was realized in the InGaAsP/InP material system. All components sketched in Fig. 4(a) are integrated monolithically on one chip. Rib waveguides are used for all components.

Fig 4(b) shows a top view of the realized matrix chip. The total length is 3.5 mm and the width amounts to 0.6 mm. The narrow dark lines correspond to straight waveguides and the curved white lines surrounded by light grey areas indicate bent waveguides. The triangles are deeply etched straylight reflectors. White rectangles indicate the contact pads. Details of the fabrication process are given in [21]. In Fig. 4(b) the optical input and output ports are marked by arrows. Coupling to single-mode fibers is performed by ball lenses as described in [22].

The central functional elements of this chip are the two crossbar switches. They are based on directional couplers which consist of two parallel waveguides with a length of 400 μm. Switching is achieved by the plasma effect due to carrier injection into one guide. The cross and the bar states are selected by turning the controlling current on and off respectively. A detailed description of the current controlled directional coupler switch is given in [23]. The combiners are based on directional couplers as well. In this case the length of the parallel waveguides amounts to 175 μm resulting in a 3dB optical power splitting.

Fig. 4(c) depicts the operation of the switching matrix. It shows infrared images of the output of the chip when light of 1.55-μm wavelength is coupled into one input waveguide and current is applied to the relevant directional coupler switch. Light is launched under 45° polarization angle into the input waveguides. The two adjacent white dots in each picture represent the two output ports of a 3-dB coupler.

It can be seen clearly that a very low control current of only 10 mA is sufficient to switch the directional coupler from the cross state to the bar state. Crosstalk in both switching states is less than 15 dB. Insertion loss amounts to 12 dB excluding fiber/chip coupling. Preliminary speed measurements showed rise and fall times of only 2 ns. It should be mentioned that
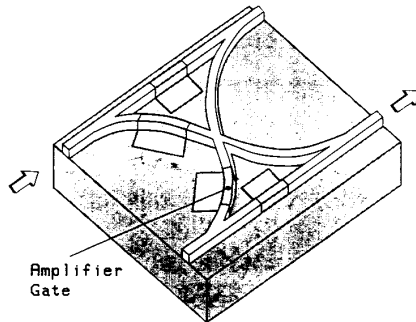
Fig. 5. Schematic representation of a 2 × 2 optical amplifier switch.

Fig. 6. Optical chip gain versus bias current for TE- and TM-polarized input light at 1.55 μm wavelength and −30 dBm input power; Insert: Schematic structure of a tilted buried-facet optical amplifier.

the experimental data given above always correspond to the worst case of both TE and TM polarization demonstrating the polarization independent operation of the realized switching matrix.

2) Amplifier Matrix: An optical gate switching matrix which consists of optical gates and optical branching circuits, is promising for a space switching stage [24]. Traveling-wave laser amplifiers are particularly effective as optical gates because of their amplification characteristics, high ON/OFF ratio, and potential for sub-nanosecond switching speed.

Fig. 5 shows a schematic representation of a possible arrangement for a monolithically integrated 2 × 2-amplifier matrix, which can be operated as crossbar or distribution switch. An optical signal launched into one of the input waveguides passes a first Y-junction and is fed to one of the two exit waveguides via an optical amplifier gate and a second Y-junction.

The inset of Fig. 6 shows a semiconductor optical amplifier structure [25] currently considered for integration into the matrix. It consists of a 1.55- μm bulk InGaAsP/InP buried heterostructure with $0.4 \times 0.8 \mu m^2$ InGaAsP crossection, providing polarization insensitive optical gain in a large (50 nm) wavelength span.

Fig. 6 shows the optical gain versus bias current. A 20-dB gain is achieved at 50-mA bias current, with less than 1-dB TE/TM gain difference and less than 1-dB wavelength dependent gain ripple. An ON/OFF ratio of more than 20 dB is realized by a current change of 30 mA. Preliminary measurements [26] of the dynamic switching characteristics reveal less than 1 ns rise and fall times for a 40 mA current step over a relatively large range of bias currents.

The observed polarization-insensitive gain and relatively fast switching characteristics make this buried heterostructure optical amplifier particularly suited as active building block of the space division switch shown in Fig. 5.

III. SYSTEM CONTROL

A. Frequency Stabilization

Three different frequency stabilization schemes providing both relative and absolute stabilization have been investigated for possible implementation in the demonstrator [27]. By modifying standard stabilization techniques the amount
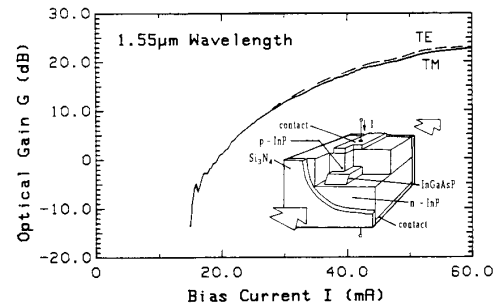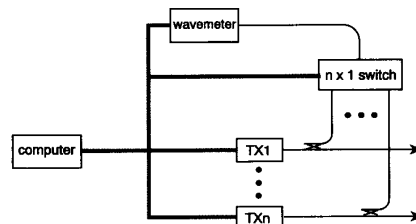

Fig. 7. Experimental setup for frequency stabilization using a wavemeter.

of hardware could be reduced considerably while sufficient stability was maintained even for channel spacings as low as 5 GHz.

A very simple scheme uses a commercial wavemeter for both relative and absolute frequency stabilization [28]. The principle of a wavemeter stabilization is shown in Fig. 7. Small fractions of the transmitter laser output signals are cyclically fed to the wavemeter by an $n \times 1$ fiber-optic switch (alternative choices are possible, if needed, for higher reliability). The current frequency is measured and a correction is applied to the transmitter under investigation. To reduce the uncertainty on the wavelength measurement result, the mean of 10 measurements is calculated and a correction proportional to the measured frequency deviation is applied to each transmitter. Due to averaging a stabilization cycle for one transmitter takes about 2.6 s.

In an experiment two transmitters were FSK-modulated at 140 Mb/s and stabilized to the nominal frequencies 192.1650 and 192.1754 THz, respectively. For testing channel spacing stability the beat signal between the two transmitters was detected in a wideband-receiver. The lower trace of Fig. 8 shows the central lobe of the beat spectrum around 10.4 Ghz. The upper trace was recorded in the maximum-hold mode during 20 h of operation. After vertical translation of the trace we had a horizontal widening of the lobe of $<\pm 50$ MHz. The center of the lobe differs from 10.4 GHz by -120 MHz due to finite wavemeter accuracy. The channel frequencies were also recorded during operation. Fig. 9 shows an error histogram where the frequency deviation from the desired frequency and the number of measurement cycles are displayed for the two transmitters. From Fig. 9 we read a maximum
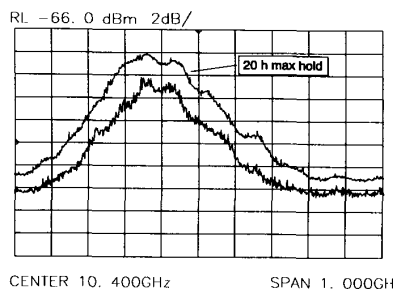
Fig. 8. Central lobe of beat spectrum between two FSK-modulated optical transmitters stabilized by a wavemeter. The frequency spacing was set to 10.4 GHz.
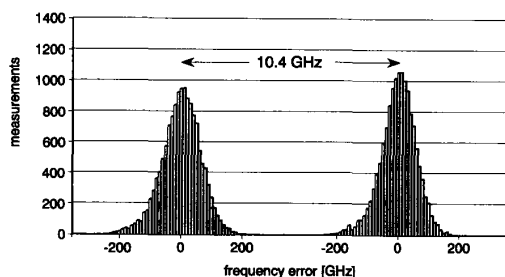

Fig. 9. Histogram of recorded frequency deviations from the desired value.

deviation of ± 250 MHz, with standard deviations of about 60 MHz.

In addition we have investigated a modified heterodyne spectroscopy stabilization scheme using a standard heterodyne receiver for relative frequency stabilization and we have performed experiments on frequency locking to an optical frequency comb generated by means of a resonant $LiNbO_3$ phase modulator. In both experiments a commercial wavemeter was used to obtain an absolute frequency stability. The channel spacing stabilities obtained were ± 50 MHz for the modified heterodyne and ± 40 MHz for the comb stabilization scheme, respectively. The maximum frequency errors measured were ± 120 MHz with standard deviations of < 25 MHz for both channels.

Considering the achieved frequency stabilities, all three schemes are suited for implementation in the demonstrator.

B. Channel Identification

To ensure that a coherent receiver has locked onto the correct channel, a channel identification procedure has been developed and tested. After channel locking the transmitter frequency is swept by laser current changes over ± 500 MHz. The AFC in the receiver tracks the transmitter frequency sweep. In a stand-alone setup the microprocssor in the receiver would identify the currently received transmitter from its sweep frequency or width. In our case of a spatially concentrated frequency conversion stage overall control of both transmitters and receivers is exerted by a personal computer so that a similar analysis is carried out by this controller.

Due to a sufficiently high bandwidth of the AFC circuit in the receiver the transmitter frequency sweep does not cause a sensitivity penalty. Sweeping is recognized from changes in the AFC output voltage that is fed back to the LO. The required time for channel identification is about 2 s. If needed, this value could be lowered by software changes.

Alternatively, a small frequency modulation with a frequency well above the AFC bandwidth could be employed and the frequency discriminator output voltage would be observed. This option, while requiring slight hardware changes, would reduce the channel identification time down to tens of ms or less. The successful operation of this type of channel identification scheme has already been demonstrated [29].

C. Overall Control

Overall system control including frequency stabilization is performed by a personal computer. The various subsystems are equipped with a microprocessor and an IEEE-488 interface which allows for a very flexible control of the whole demonstrator. The local intelligence in the various subsystems is written in Forth, and provides the specific commands which are necessary to control the lasers or switching matrices respectively. The overall control software is written in Pascal. Optical frequency stabilization is performed in a background routine.

We shall discuss here the response of the system to frequency switching commands. Using a setup of two frequency-stabilized transmitters (5.5-GHz channel spacing) and a receiver we have conducted experiments to verify correct channel locking of a DIPS receiver. The receiver was locked alternately to the two channels, 25 000 times for each of them. Polarization in the standard single-mode transmission fiber was changed repeatedly in order to ensure that channel acquisition would be tested for all possible polarization states, including the most difficult cases. Since the frequency deviation of the FSK transmitter is 1.2 GHz, incorrect locking would occur at an LO frequency 1.2 GHz above or below the expected value. Not a single incorrect locking was observed among the 50 000 channel acquisition procedures.

Our receivers lock always to the channel that is nearest to the frequency at which it is supposed to be. Even if a much stronger channel is only slightly farther away the nearest channel is still correctly detected. The algorithm allows reliable operation of the demonstrator even if the frequency stabilization should ever fail. Fig. 10 plots the time needed for channel acquisition in a DIPS receiver as a function of the positive or negative frequency offset between expected and actual transmitter frequencies. For offsets up to 3 GHz the locking time is < 0.7 s. For higher offsets the time increases because the microprocessor of the receiver will undertake more and wider LO frequency sweeps until the nearest channel is found. Although the data points of Fig. 10 may look unpredictable they are in fact deterministic and reflect exactly the search program execution.

As already mentioned in Section II-B, channel acquisition in a polarization diversity receiver is accomplished somewhat faster because the number of final LO frequency sweeps is 1 rather than 15.
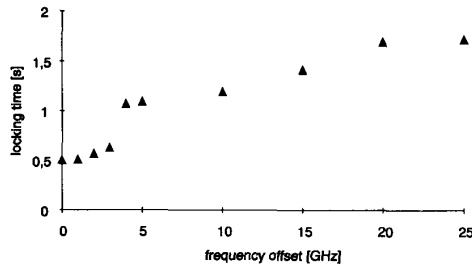
Fig. 10.   Time needed for channel acquisition in a DIPS receiver as a function of the positive or negative frequency offset between expected and actual transmitter frequencies.

At any desired moment the overall control program can send out commands to establish a desired link.

IV. CONCLUSIONS

We have presented the concept of an OFDM switching node suitable for flexible interconnection of future IBC nodes. Our demonstrator will consist of a frequency switching stage composed of tunable FSK heterodyne receivers which are permanently connected to tunable FSK transmitters. A subsequent InP space switching stage, consisting of directional coupler switches or gate switching matrices based on optical amplifiers, will allow to switch the channels to any desired output fiber. As of now we have established the basic functions necessary for frequency stabilization, frequency switching and space switching. Completion of the demonstrator by additional equipment, namely the space switching matrices, is expected in the near future.

ACKNOWLEDGMENT

The authors would like to thank G. J. Valentine (Bath University) and V. Bodlaj for their work on software, optical transmitters and optical receivers, G. Kristen and S. Pröhl for providing the optical amplifiers, and B. Bauer for his optical gain measurement. The authors alone are responsible for the contents.

REFERENCES

[1] H. M. Foisel, E. J. Bachus, R. P. Braun, C. Caspar, and B. Strebel, "Coherent OFDM switching systems," in *Proc. EFOC/LAN '90,* 1990, pp. 347–351.
[2] M. Fujiwara *et al.,* "A coherent photonik wavelength-division switching system for broadband networks," *Proc. ECOC '88,* vol. 1, 1988, pp. 139–142.
[3] P. Healey *et al.,* "Demonstration of the MONET extendible optical switch fabric," in *Proc. ECOC '91,* vol. 1, 1991, pp. 169–172.
[4] H. H. Witte, "Novel photonic switching network using optical frequency-division shared-medium switches," *Proc. Int. Topical Meeting on Photonic Switching,* Minsk, paper 2C4, 1992.
[5] R. Noé *et al.,* "Fully engineered coherent multichannel transmitters and receivers with low-cost potential," *Electron. Lett.,* vol. 28, pp. 14–15, 1992.
[6] S. Illek, W. Thulke, C. Schanen, H. Lang, and M.-C. Amann, "Over 7 nm (875 GHz) continuous wavelength tuning by tunable twin-guide laser diode," *Electron. Lett.,* vol. 26, pp. 46–47, 1990.
[7] P. I. Kuindersma *et al.,* "Tunable three-section, strained MQW,PA-DFB's with large single mode tuning range (71Å) and narrow linewidth (around 1 MHz)", *Proc. IEEE Int. Semiconductor Laser Conf.* (Davos), paper M.4, 1990.

[8] H. Nishinoto, M. Iwasaki, S. Suzuki, and M. Kondo, "Polarization independent LiNbO₃ 8 × 8 matrix switch," *IEEE Photon. Technol. Lett.,* vol. 2, pp. 634–636, 1990.
[9] P. W. Hooijmans, M. T. Tomesen, and A. van de Grijp, "Biphase linecoding in optical FSK heterodyne transmission experiment, without sensitivity degradation compared to NRZ," *Electron. Lett.,* vol. 25, pp. 326–328, 1989.
[10] G. Grosskopf, R. Ludwig, and H. G. Weber, "140 Mbit DPSK transmission using an all-optical frequency converter with a 4000 GHz conversion range," *Electron. Lett.,* vol. 24, pp. 1106–1107, 1988.
[11] S. Murata, A. Tomita, J. Shimizu, and A. Suzuki, "THz optical frequency conversion of 1 Gb/s signals using highly nondegenerate four-wave mixing in semiconductor lasers," *Proc. IOOC/ECOC '91,* vol. 1, pp. 85–88, 1991.
[12] O. Hildebrand *et al.,* "The integrated interferometric injection laser (Y-Laser): One device concept for various system applications," *Proc. IOOC/ECOC '91,* vol. 2, 1991, pp. 39–46.
[13] R.-P. Braun, E.-J. Bachus, C. Caspar, H.-M. Foisel, and B. Strebel, "Transparent all-optical coherent multi-carrier 4 × 2 switching node," *Proc. IOOC/ECOC '91,* vol. 3, 1991, pp. 92–95.
[14] B. Glance *et al.,* "Broadband optical wavelength shifter," *Conf. on Lasers and Electro-Optics (CLEO'92),* 1992, paper CPD 27.
[15] B. Glance *et al.,* "High performance optical wavelength shifter," *Electron. Lett.,* vol. 28, pp. 1714–1715, 1989.
[16] T. Durhuus *et al.,* "High-speed all-optical gating using a two-section semiconductor optical amplifier structure," *Conf. on Lasers and Electro-Optics (CLEO'92),* 1992, paper CThS4.
[17] F. Ebskamp *et al.,* "Heterodyne detection of wavelength converted CPFSK signals up to 4.8 Gbit/s," *Proc. ECOC'92,* vol. 3, 1992, pp. 871–874.
[18] R. Noé *et al.,* "Comparison of polarization handling methods in coherent optical systems," *J. Lightwave Technol.,* vol. 9, pp. 1353–1366, 1991.
[19] R. Noé, J. L. Gimlett, R. S. Vodhanel, and S. Tsuji, "Polarization-insensitive, 500 Mbit/s FSK transmission over 153 km by passive polarization switching," *Electron. Lett.,* vol. 25, pp. 4–5, 1989.
[20] K. Noguchi, T. Sakano, and T. Matsumoto, "A 128 × 128 -channel free-space optical switch using polarization multiplexing technique," *Proc. IOOC/ECOC '91,* vol. 1, 1991, pp. 165–168.
[21] L. Stoll *et al.,* "4 × 4 Optical matrix switch on InP with low switching current," *AEÜ,* vol. 46, pp. 116–118, 1992.
[22] A. Greil, H. Haltenorth, and F. Taumberger, "Optical 4 × 4 InP switch module with fiber-lens-arrays for coupling," *Proc. ECOC'92,* vol. 1, 1992, pp. 529–532.
[23] L. Stoll *et al.,* "Compact and polarization independent optical switch on InP/InGaAsP," *Proc. ECOC'92,* vol. 1, 1992, pp. 337–340.
[24] M. Janson *et al.,* "Monolithically integrated 2 × 2 InGaAsP/InP laser amplifier gate switch arrays," *Electron. Lett.,* vol. 28, pp. 776–778, 1992.
[25] R. Schimpe *et al.,* "1.5 µm InGaAsP tilted buried-facet optical amplifier," *Conf. on Lasers and Electro-Optics (CLEO'91),* 1991, paper CFK5.
[26] H. Hedrich and R. Schimpe, Unpublished results.
[27] R. Noé, A. Ebberg, and B. Noll, K. Drögemüller, "Optical frequency stabilization schemes for coherent multichannel applications," *Proc. EFOC/LAN '92,* 1992, pp. 350–354.
[28] M. J. Creaner *et al.,* "Field demonstration of a two channel coherent transmission with a diode-pumped fiber amplifier repeater," *Electron. Lett.,* vol. 26, pp. 1621–1623, 1989.
[29] Q. Jiang, "Channel selection and identification for coherent optical FDM systems," *IEEE Photon. Technol. Lett.,* vol. 3, pp. 767–768, 1991.

Alfred Ebberg was born in Hemer, West Germany, in 1955. He received teh Dipl. Ing. and the Dr. Ing. degrees, both in electrical engineering, from the Ruhr University of Bochum, West Germany, in 1982 and 1988, respectively.

From 1982 to 1987 he was a Research Assistant at the Lehrstuhl für Allgemeine Elektrotechnik und Elektrooptik, Ruhr University of Bochum, where he was engaged in research on fiber-optic rotation sensing. In 1987 he joined Siemens Research Laboratories in Munich. His current interests are coherent optical communication systems.

Reinhold Noé was born in Darmstadt, West Germany, in 1960. He received the M.S. and Ph.D. degrees in electrical engineering from the Technical University of Munich, Germany, in 1984 and 1987, respectively. His doctoral thesis was mainly on endless polarization control.

He spent one postdoctoral year at Bellcore, Red Bank, NJ. His contributions to this paper originate from his employment at the Siemens Research Laboratories in Munich, Germany, from 1988 to 1992. Since autumn of 1992 he has been a Full Professor at the University of Paderborn, Germany, Department of Electrical Engineering, heading the Chair of Optical Communications. His area of interest has been, and continues to be, applied research on optical communication systems.
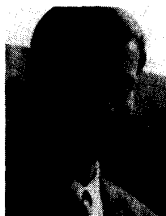
Lothar Stoll was born in Osnabrück, Germany, in 1958. He received the Diploma degree in physics from the University of Münster in 1986, where he was specially engaged in picosecond optoelectronics and optoelectronic microwave generation.

In 1986 he joined the research labs of the SIEMENS AG in Munich, Germany, working firstly on the development of projection lithography processes for integrated optical components. Since 1988 he has been concerned with the design and realization of optical waveguide switches in the InGaAsP material system.

Mr. Stoll is a member of the German Physical Society (DPG).

Robert Schimpe (M'86) was born in Munich, Germany, in 1953. He received the Dipl.-Ing. degree in 1979, and the Dr.Ing. degree with "summa cum laude" in 1984, both from the Technical University of Munich, Germany. His dissertation project was on amplitude and phase noise of index-guided GaAs laser diodes.

In 1985, he was a Guest Scientist at AT&T Bell Laboratories, Holmdel, NJ, where he investigated the modulation properties of InGaAsP laser diodes by a heterodyne detection technique. In 1986, he joined the Research Laboratories of the Siemens AG, Munich, as a member of the department for optoelectronic semiconductor devices. Presently, he is engaged in the field of InP-based OEIC's and of optical amplifiers and switches, in particular. He holds several patents and published more than 20 scientific papers.

Dr. Schimpe is corecipient of the NTG Preis of the Nachrichtentechnische Gesellschaft in the Verband Deutscher Elektrotechniker (VDE) for his contribution to the theory of laser intensity noise in 1984.